Effects of a Non-Uniform Radial Load Distribution on Stress Field in Brazilian Tests

A.Lavrov

A.Vervoort

Catholic University Leuven, Faculty of Applied Sciences
Department of Civil Engineering, Mining Division
Kasteelpark Arenberg 40, B-3001, Leuven, Belgium
Tel.: +32 16 32 16 65
Fax: +32 16 32 19 88
E-Mail: alexander.lavrov@bwk.kuleuven.ac.be
andre.vervoort@ bwk.kuleuven.ac.be

ABSTRACT

A general solution for stress distribution in a disk loaded by radial stresses applied over two opposite arcs shows that the direction of principal axes in the points of the main diameter near the loaded arcs can be different from this diameter. For regular sine-type fluctuations of σ_{rr} , the zone of their influence approaches the loaded arcs when the frequency of fluctuations increases. This can lead to higher stress gradients in the vicinity of the loaded arcs to cause complicated fracture paths in these areas. The influence of high-frequency oscillations of σ_{rr} (about 100 sine-wave lengths on the loaded arc) on the orientation of principal axes in the points of the main diameter is negligible both in central and peripheral parts of the disk. Low-frequency oscillations (<10 sine-wave lengths on the loaded arc) can significantly contribute to the stress distribution and principal axes orientation in the vicinity of the contacts. The deviation of the principal axis from perpendicular to the main diameter is about 30º in the vicinity of the loaded arcs, if the amplitude of the load oscillation is 10% of the main load. This angle increases to approximately 40º with increasing amplitude of the oscillation. Together with higher stress gradients, this must contribute to complicated fracture paths in the vicinity of the disk-platen contacts. The influence of low-frequency oscillations on the orientation of principal axes in the central part of the main diameter is negligible. The results confirm the relatively consistent fracture mode observed in Brazilian tests.

Key Words: Brazilian test, load fluctuation, tensile strength, fracture.

1. INTRODUCTION

Brazilian test is one of the most widespread methods for indirect tensile strength measurement of rocks. The method involves compressive loading of a rock disk in the direction of one of its diameters, which is called the main diameter in the following text (Fig.1a). Along a part of the main diameter, tensile stress acts in the direction perpendicular to the diameter. This tensile stress induces a tensile fracture (macro-crack) which is usually believed to propagate when the tensile stress reaches the tensile strength of rock. The crack propagates in an unstable manner along approximately the main diameter or with some deviations (Fig.1b) (Jaeger and Cook, 1969).

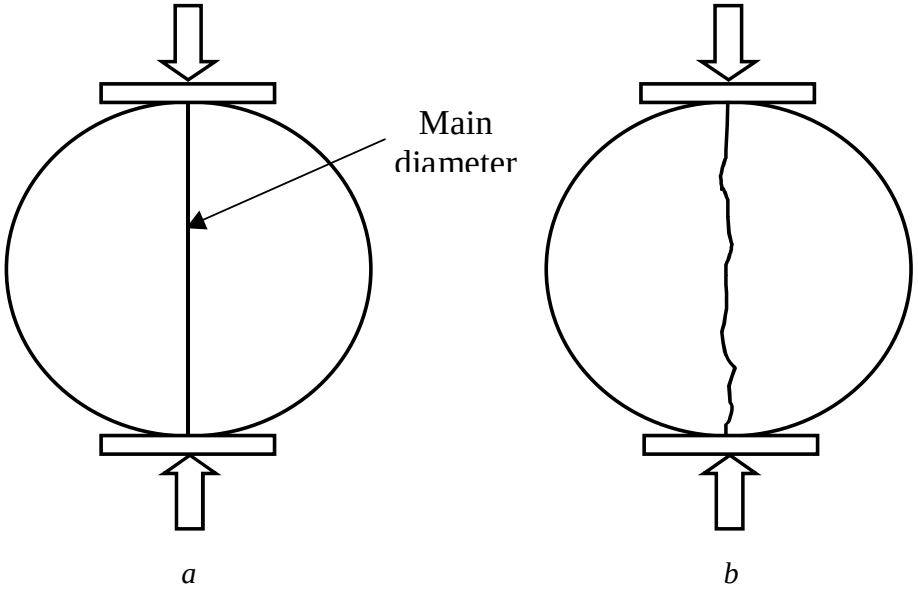

Fig. 1: Disk-shaped rock sample between loading platens

Since it was proposed, the Brazilian test has proved to be a simple, fast and relatively reliable technique for tensile strength estimation of rocks. It is widely used in rock mechanics laboratories all over the world both in research work and routine tests. During the test, a rock specimen is loaded either between the platens of the testing machine without any inserts, between specially designed jaws (Bieniawski and Hawkes, 1978), or hardboard inserts are placed between the disk circular boundary and the loading platens to make the load distribution more or less uniform (Colback, 1966; Van de Steen and Wevers, 1998; Van de Steen et al., 1998). The use of different types of load distributors can give rise to rather complicated fracture paths in Brazilian tests (Colback, 1966).

For the calculation of the tensile strength from the measured ultimate compressive load, results of the linear elastic computation of the stress field in a disk are used. In the commonly used exact solution of the theory of elasticity, stress distributions at the upper and bottom boundaries of the disk are assumed either in the form of point loads or uniformly distributed (constant) radial

pressure (Fairhurst, 1964; Colback, 1966; Jaeger and Cook, 1969; Chen et al., 1998). By using numerical simulations, other load distributions like for example trapezoidally distributed load have been employed (Van de Steen, 1999).

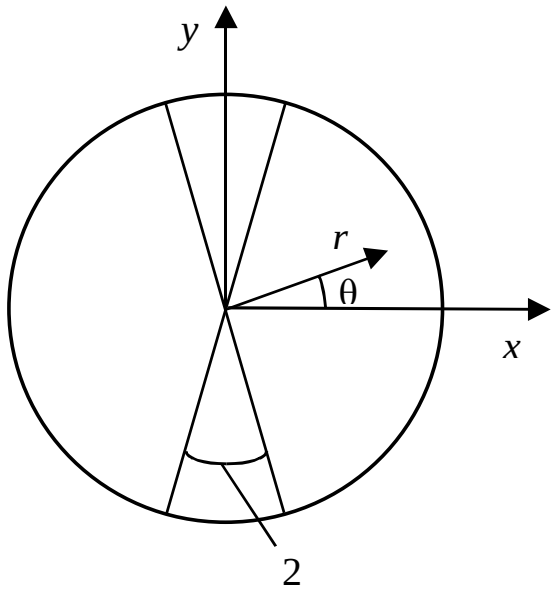

Fig. 2 : Polar (r, θ) and Cartesian (x, y) coordinate systems; 2β indicates the arc over which the applied load is distributed

In case of a disk of radius R=1 loaded by uniform (constant) normal stress P applied over two opposite arcs 2β, the stresses in the points of the main diameter (θ=π/2) are given in Cartesian coordinates (Fig.2) by (Jaeger and Cook, 1969)

$$\sigma_{xx} = -\frac{2P}{\pi}\left\{\frac{(1-r^2)\sin 2\beta}{1-2r^2\cos 2\beta + r^4} - \tan^{-1}\left[\frac{1+r^2}{1-r^2}\tan\beta\right]\right\}$$

(1)
$$\sigma_{yy} = \frac{2P}{\pi}\left\{\frac{(1-r^2)\sin 2\beta}{1-2r^2\cos 2\beta + r^4} + \tan^{-1}\left[\frac{1+r^2}{1-r^2}\tan\beta\right]\right\}$$

$$\sigma_{xy} = 0$$

Here and in the following text, tensile stresses are positive as it is usually adopted in the theory of elasticity. The applied compressive load P in the Brazilian test is negative.

In rock mechanics practice, the applied load distribution can differ from uniform, and can be characterized by irregular variations of radial stress around

a certain mean value. This can be due for example to the roughness of the sample circumference or of the inserts, to the granular structure and, hence, elastic inhomogeneity of rock, or to the inhomogeneity of the inserts with respect to their elastic properties. It is often believed that radial stress fluctuations do not effect the stress field in the major part of the disk (Fairhurst, 1964). The aim of this paper is to verify this assumption in an analytical way as well as to estimate the effect of the radial stress oscillations on the stress distribution and principal axes orientation in the fracture zone along the main diameter.

2. SOLUTION FOR GENERAL TYPE OF σ_{rr} –FLUCTUATION AROUND A ZERO LEVEL

Consider a disk of radius R=1 loaded over two opposite arcs by distributed radial stresses as follows:

$$\sigma_{rr} = \begin{cases} 0 \text{ for } 0 \le \theta \le \frac{\pi}{2} - \beta; \frac{\pi}{2} + \beta \le \theta \le \frac{3\pi}{2} - \beta; \frac{3\pi}{2} + \beta \le \theta \le 2\pi \\ f(\theta - \frac{\pi}{2}) \text{ for } \frac{\pi}{2} - \beta \le \theta \le \frac{\pi}{2} + \beta \\ f(\theta - \frac{3\pi}{2}) \text{ for } \frac{3\pi}{2} - \beta \le \theta \le \frac{3\pi}{2} + \beta \end{cases} \tag{2}$$

Here, r and θ refer to the polar coordinate system; 2β is the arc loaded (Fig.2). Positive values of $f(\theta)$ correspond to tension. For the sake of simplicity, the distribution of σ_{rr} is assumed to have central symmetry as it is seen from Eq. (2). Moreover, assume $f(-\beta)=f(\beta)=0$ and $\int_{-\beta}^{\beta} f(\psi)d\psi = 0$. The latter equation means that only stress deviations from the average value are considered, with the mean value being zero.

Find the stress field satisfying the boundary condition (2), using complex potentials method. Stresses in Cartesian coordinates (Fig.2) can be expressed through the complex potentials $\varphi(z)$ and $\psi(z)$, being analytic functions of the complex variable z, as follows (Muskhelishvili, 1963):

$$\begin{aligned} \sigma_{xx} + \sigma_{yy} &= 4\,\mathrm{Re}\,\varphi'(z) \\ \sigma_{yy} - \sigma_{xx} + 2i\sigma_{xy} &= 2\left[\bar{z}\varphi''(z) + \psi'(z)\right] \end{aligned} \tag{3}$$

where $z=x+iy=re^{i\theta}$ and x, y are Cartesian coordinates as shown in Fig. 2. Re refers to the real part of the expression by which it is followed.
The main vector of the forces acting on the boundary is equal to zero. Hence, the potentials $\varphi(z)$ and $\psi(z)$ are holomorphic functions and can be represented by Laurent expansions as follows:

(4) $$\varphi(z) = \sum_{k=0}^{+\infty} a_k z^k$$

(5) $$\psi(z) = \sum_{k=0}^{+\infty} b_k z^k$$

Let the boundary condition (2) be expanded as a complex Fourier series:

(6) $$\sigma_{rr}\big|_{r=1} = \sum_{k=-\infty}^{+\infty} \alpha_k e^{ik\theta}$$

where $\alpha_k = \frac{1}{2\pi}\int_{-\beta}^{\beta} \sigma_{rr}(\psi) e^{-ik\psi} d\psi$. Due to the above-described properties of $\sigma_{rr}(\theta)$, $\alpha_0 = 0$, $\alpha_{2m+1} = 0$, $\alpha_{2m} = (-1)^m \cdot \frac{1}{\pi}\int_{-\beta}^{\beta} f(\psi) e^{-2im\psi} d\psi$. Thus Fourier expansion of the fluctuation function is given by

(7) $$\sigma_{rr}\big|_{r=1} = \sum_{m=-\infty}^{-1} \alpha_{2m} e^{2im\theta} + \sum_{m=1}^{+\infty} \alpha_{2m} e^{2im\theta}$$

Calculating the derivatives of $\varphi(z)$ and $\psi(z)$ and substituting them in the boundary condition (Muskhelishvili, 1963)

(8) $$\sigma_{rr}\big|_{r=1} = \varphi'(z) + \overline{\varphi'(z)} - \left[\bar{z}\varphi''(z) + \psi'(z)\right] e^{2i\theta}$$

results in the equation for finding coefficients a_k, b_k:

(9) $$\sum_{m=-\infty}^{-1} \alpha_{2m} e^{2im\theta} + \sum_{m=-1}^{+\infty} \alpha_{2m} e^{2im\theta} = 2a_1 + \sum_{k=1}^{+\infty} (1-k^2) a_{k+1} e^{ik\theta} + \\ + \sum_{k=1}^{+\infty} (k+1) \overline{a_{k+1}} e^{-ik\theta} - \sum_{k=2}^{+\infty} (k-1) b_{k-1} e^{ik\theta}$$

When deriving (9), it was taken into account that $\varphi(0)$, $\varphi'(0)$ and $\psi(0)$ can be set equal to zero which yields immediately a_0=0, Im a_1=0 and b_0=0.

From (9), the complex potentials are derived as follows:

$$\varphi(z) = \sum_{m=1}^{+\infty} \frac{\alpha_{2m}}{2m+1} \cdot z^{2m+1}$$

(10)

$$\psi(z) = \sum_{m=1}^{+\infty} \frac{2m\alpha_{2m}}{1-2m} \cdot z^{2m-1}$$

and, hence, the stresses in Cartesian coordinates are given by:

$$\sigma_{xx} = 2\sum_{m=1}^{+\infty}(\alpha'_{2m}\cos 2m\theta - \alpha''_{2m}\sin 2m\theta)r^{2m} -$$
$$-2\sum_{m=1}^{+\infty} m(r^{2m} - r^{2m-2})[\alpha'_{2m}\cos(2m-2)\theta - \alpha''_{2m}\sin(2m-2)\theta]$$

(11)
$$\sigma_{yy} = 2\sum_{m=1}^{+\infty}(\alpha'_{2m}\cos 2m\theta - \alpha''_{2m}\sin 2m\theta)r^{2m} +$$
$$+2\sum_{m=1}^{+\infty} m(r^{2m} - r^{2m-2})[\alpha'_{2m}\cos(2m-2)\theta - \alpha''_{2m}\sin(2m-2)\theta]$$

$$\sigma_{xy} = 2\sum_{m=1}^{+\infty} m(r^{2m} - r^{2m-2})[\alpha''_{2m}\cos(2m-2)\theta + \alpha'_{2m}\sin(2m-2)\theta]$$

where $\alpha'_{2m} = \mathrm{Re}\,\alpha_{2m}$, $\alpha''_{2m} = \mathrm{Im}\,\alpha_{2m}$.

For an even function $f(\theta)$, σ_{xy} is zero along the main diameter (y-axis), i.e. for $\theta=\pi/2$. However, in the reality, the distribution of the radial load over the loading arcs may be arbitrary. E.g. for an odd function $f(\theta)$, it follows from (11) that $\sigma_{xx}=\sigma_{yy}=0$ along y-axis, but the shear stress σ_{xy} can be different from zero and be given by

(12)
$$\sigma_{xy} = 2\sum_{m=1}^{+\infty}(-1)^{m+1} m(r^{2m} - r^{2m-2})\alpha''_{2m}$$

In the center of the disk $\sigma_{xy}=-2\alpha''_2$. This means that in a general case of σ_{rr}–fluctuation, the direction of the principal axes in the points of the main diameter (y-axis) can be different from this diameter. The extent of this influence in different parts of the main diameter will be estimated in the next section for a particular case of σ_{rr}–fluctuation given by a sine-function.

3. PARTICULAR CASE OF σ_{rr}–FLUCTUATION: SINE-OSCILLATION

In order to illustrate the influence of σ_{rr}–fluctuations on the stress distribution and principal axes orientation in the disk, consider a particular case of fluctuation, namely that of sine-type. In this case, the boundary condition (1) can be re-written as follows:

$$\sigma_{rr} = \begin{cases} 0 \text{ for } 0 \le \theta \le \frac{\pi}{2} - \beta; \frac{\pi}{2} + \beta \le \theta \le \frac{3\pi}{2} - \beta; \frac{3\pi}{2} + \beta \le \theta \le 2\pi \\ p \sin \frac{\pi n}{\beta} \left(\theta + \beta - \frac{\pi}{2} \right) \text{for } \frac{\pi}{2} - \beta \le \theta \le \frac{\pi}{2} + \beta \\ p \sin \frac{\pi n}{\beta} \left(\theta + \beta - \frac{3\pi}{2} \right) \text{for } \frac{3\pi}{2} - \beta \le \theta \le \frac{3\pi}{2} + \beta \end{cases} \tag{13}$$

Here, p has the meaning of the oscillation amplitude. Equation (13) implies that n wave lengths are contained within the loading arc of 2β. $\sigma_{rr}(\theta)$ given by (13) is continuous in all points. In its Fourier-expansion, all α'_{2m} are equal to zero, and the stresses σ_{xx}, σ_{yy}, σ_{xy} as derived from (6), (11) and (13) are:

$$\sigma_{xx} = \sum_{m=1}^{+\infty} (-1)^m \cdot \frac{4pn\beta \sin 2m\beta}{4m^2\beta^2 - \pi^2 n^2} \cdot [r^{2m} \sin 2m\theta - \\ - mr^{2m} \sin(2m-2)\theta + mr^{2m-2} \sin(2m-2)\theta]$$

$$\sigma_{yy} = \sum_{m=1}^{+\infty} (-1)^m \cdot \frac{4pn\beta \sin 2m\beta}{4m^2\beta^2 - \pi^2 n^2} \cdot [r^{2m} \sin 2m\theta + \\ + mr^{2m} \sin(2m-2)\theta - mr^{2m-2} \sin(2m-2)\theta] \tag{14}$$

$$\sigma_{xy} = \sum_{m=1}^{+\infty} (-1)^m \cdot \frac{4pmn\beta \sin 2m\beta}{4m^2\beta^2 - \pi^2 n^2} \cdot \left(r^{2m-2} - r^{2m} \right) \cos(2m-2)\theta$$

Along the main diameter ($\theta=\pi/2$), $\sigma_{xx}=\sigma_{yy}=0$. The shear stress σ_{xy} is different from zero along the main diameter. Its value in the center of the disk is given by

$$\sigma_{xy}\big|_{r=0} = \frac{4pn\beta \sin 2\beta}{\pi^2 n^2 - 4\beta^2} \tag{15}$$

E.g. for p=10MPa, β=11˚, n=1 σ_{xy}=0.3 MPa. For p=10MPa, β=11˚, n=10 σ_{xy}=0.03 MPa. Hence, even for the smallest value of n, the shear stress in the center of the disk does not exceed several percent of the amplitude of the σ_{rr}–fluctuation on the boundary.

The shear stress value given by (15) increases with increasing loading angle β. It can also be concluded from (15) that, with increasing *n*, σ_{xy} in the center reduces. This means that with intensifying frequency of σ_{rr}–fluctuations on the boundary, their influence on the stress distribution and orientation of principal axes in the central part of the disk decreases. This conclusion is illustrated in Figures 3 and 4 where stress distributions along the main diameter are plotted for *n*=2 and *n*=8, respectively. Figures 3 and 4 show that with increasing frequency of fluctuations measured by *n*, the zone of influence reduces dramatically and approaches the loaded arc of the circular boundary. The magnitude of the stress field perturbation all over the disk decreases substantially with increasing *n*. For instance, for *n*=2 the maximum absolute value of σ_{xy} on the main diameter is of the same order as the fluctuation amplitude *p* (Fig.3). For *n*=100, the maximum absolute value of σ_{xy} on the main diameter is by three order smaller than *p* (Fig.5). This means that the effect of high-frequency oscillations which are inevitably present in real Brazilian tests due to the inhomogeneity of the contact areas with respect to elastic properties of rock, can be neglected. This is one of the reasons why the fracture path has a relatively consistent form in Brazilian tests.

4. EFFECTS OF VARIATION OF NORMAL LOAD ON THE PRINCIPAL STRESS DIRECTION

To illustrate the influence of low-frequency oscillation on the orientation of principal axes in Brazilian disks, calculate the angle between the principal axis and the *x*-axis in the case when the sine-oscillation of amplitude *p* is superposed on the constant normal load of value *P*. The boundary condition corresponding to this case is given by:

$$\sigma_{rr} = \begin{cases} 0 \ \text{ for } 0 \le \theta \le \dfrac{\pi}{2} - \beta; \dfrac{\pi}{2} + \beta \le \theta \le \dfrac{3\pi}{2} - \beta; \dfrac{3\pi}{2} + \beta \le \theta \le 2\pi \\ P + p\sin\dfrac{\pi n}{\beta}\left(\theta + \beta - \dfrac{\pi}{2}\right) \text{for } \dfrac{\pi}{2} - \beta \le \theta \le \dfrac{\pi}{2} + \beta \\ P + p\sin\dfrac{\pi n}{\beta}\left(\theta + \beta - \dfrac{3\pi}{2}\right) \text{for } \dfrac{3\pi}{2} - \beta \le \theta \le \dfrac{3\pi}{2} + \beta \end{cases} \tag{16}$$

The angle α between the direction of the major (tensile) principal stress and the *x*-axis is defined by

$$\tan 2\alpha = \frac{2\sigma_{xy}}{\sigma_{xx} - \sigma_{yy}} \tag{17}$$

whereas α is positive anti-clockwise.

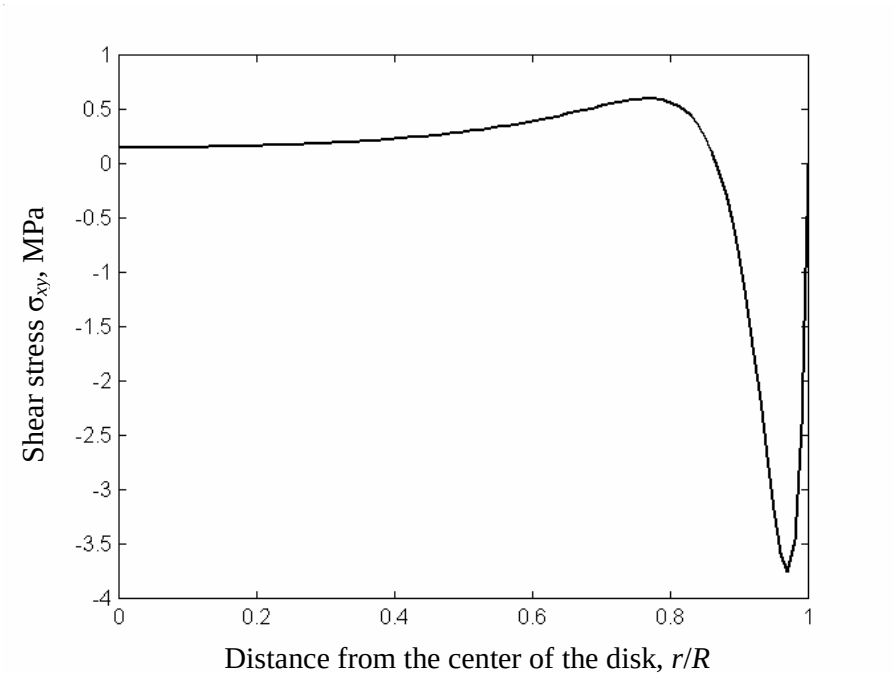

Fig. 3: Shear stress vs distance along the main diameter (p=10MPa; β=11˚; n=2)

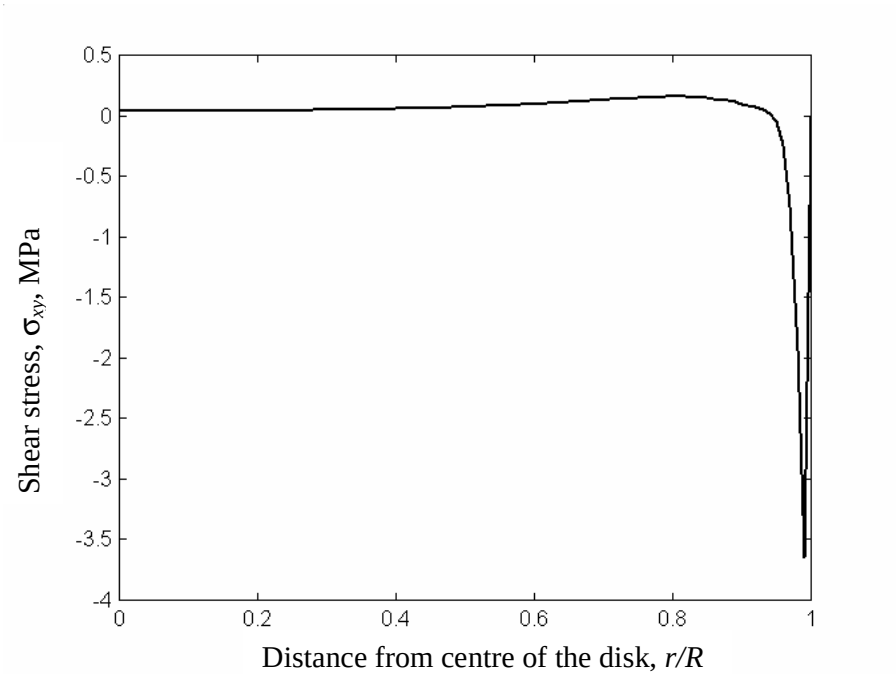

Fig. 4: Shear stress σ_{xy} vs distance along the main diameter (p=10MPa; β=11˚; n=8)

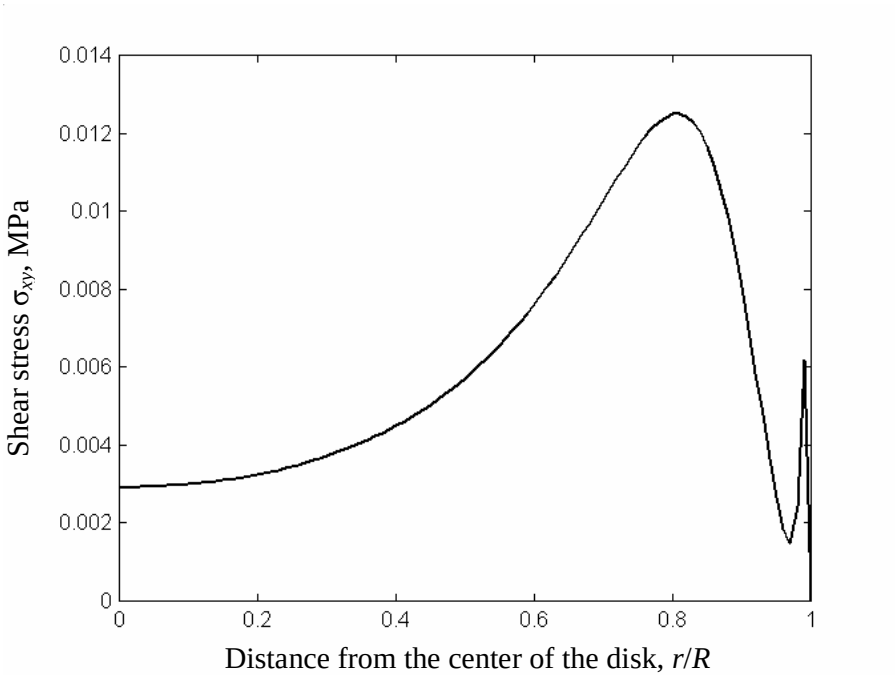

Fig. 5: Shear stress vs distance along the main diameter (p=10MPa; β=11˚; n=100)

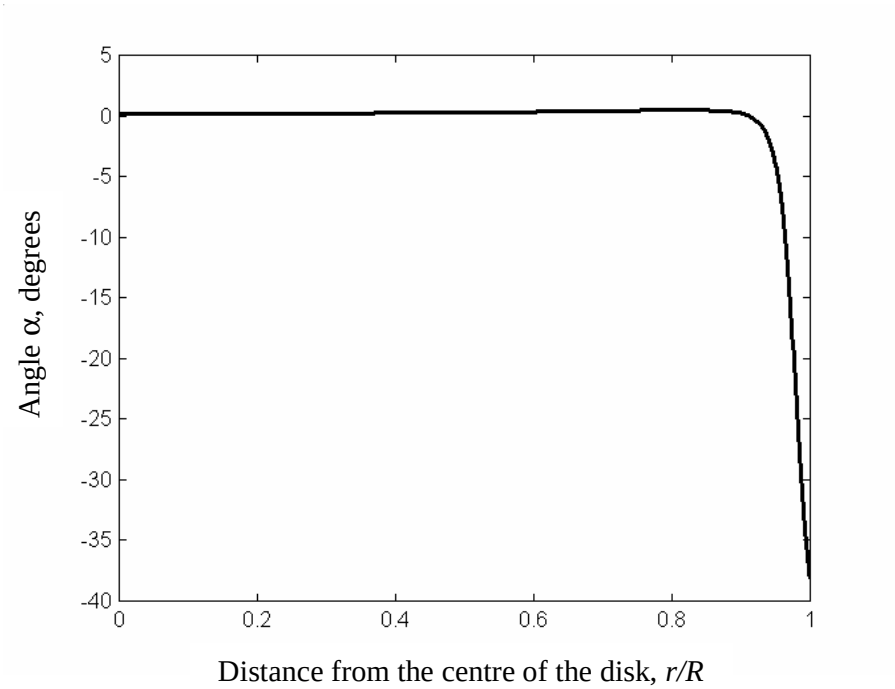

Fig. 6: Angle α between the major principal direction and the x-axis vs distance along the main diameter (P=-50 MPa; p=10MPa; β=11˚; n=4)

Superposing the solutions given by (1) and (14) in the points of the main diameter ($\theta=\pi/2$) and substituting the resulting values of stresses σ_{xx}, σ_{yy}, σ_{xy} in Eq. (17) yields:

$$\tan 2\alpha = \frac{2\pi\, pn\beta\left(1 - 2r^2\cos 2\beta + r^4\right)}{P\sin 2\beta}\sum_{m=1}^{+\infty}\frac{m\sin 2m\beta}{4m^2\beta^2 - \pi^2 n^2}r^{2m-2} \tag{18}$$

Analysis of Eq. (18) allows to conclude that the deviation of the principal direction from the *x*-axis increases with increasing ratio *p*/*P*. For *p*=0, i.e. when the normal load does not have any oscillations, the value of α is equal to zero, i.e. the principal direction is perpendicular to the main diameter in all points of it. A typical dependence of α on the radius along the main diameter is shown in Fig.6. In Fig. 6, *P* = -50 MPa, *p*=10 MPa, *n*=4, β=11˚. The dimension of the influence zone does not exceed 0.1*R*. Along the part of the main diameter where σ_{xx} is tensile, the deviation of the principal direction from the perpendicular to this diameter is negligible. The value of α increases substantially in the zone close to the loaded arc. In the example shown in Figure 6 the value of α increases to 38˚ in the narrow zone of about 0.1*R* near the arc loaded. This means that low-frequency oscillations can considerably affect the orientation of the principal axes in the narrow zone near the contacts, where both principal stresses are compressive. This, together with other factors (initial crack orientations, high compressive stresses) considered elsewhere (Colback, 1966) can lead to complicated fractures in these areas.

The absence of the influence of low-frequency oscillations on principal directions in the major (central) part of the main diameter is one more reason of the consistency of the fracture mode in Brazilian tests.

The effect of low-frequency oscillation on principal directions orientation near the contacts gradually decreases with increasing frequency of oscillations measured by *n* as well as with decreasing ratio *p*/*P*. This is illustrated by Figs. 7 and 8. Figure 7 shows that even by a relatively low oscillation amplitude of 10% of the mean value, the deviation of principal axes from the directions predicted by conventional theory (Eq. (1)) is considerable (about 30˚) in the vicinity of the contact. The deviation of principal axes from *x*,*y*-directions decreases to about 5˚ when the ratio *p*/*P* drops to 0.01 as it is seen in Fig. 8 (*n*=4, *P*=-50 MPa are the same in Figs. 6, 7 and 8). This result shows that by relative amplitude of oscillation of the order of $n\cdot 10\%$, the inclination of the principal axes in the contact areas may be quite noticeable making the fracture development in these zones even more complicated than it is usually believed.

Plotting the dependencies of σ_{rr}, $\sigma_{\theta\theta}$, $\sigma_{r\theta}$, σ_{xx}, σ_{yy}, σ_{xy} versus radius for different values of θ (i.e. along diameters inclined to the main diameter of the disk) shows that the dimension of the influence zone (measured as a distance from the loaded arcs) and the magnitude of the stress deviations from the values predicted by conventional theory (Eq. (1)) along these diameters unambiguously reduce with increasing *n*. The deviations of stresses σ_{rr}, $\sigma_{\theta\theta}$

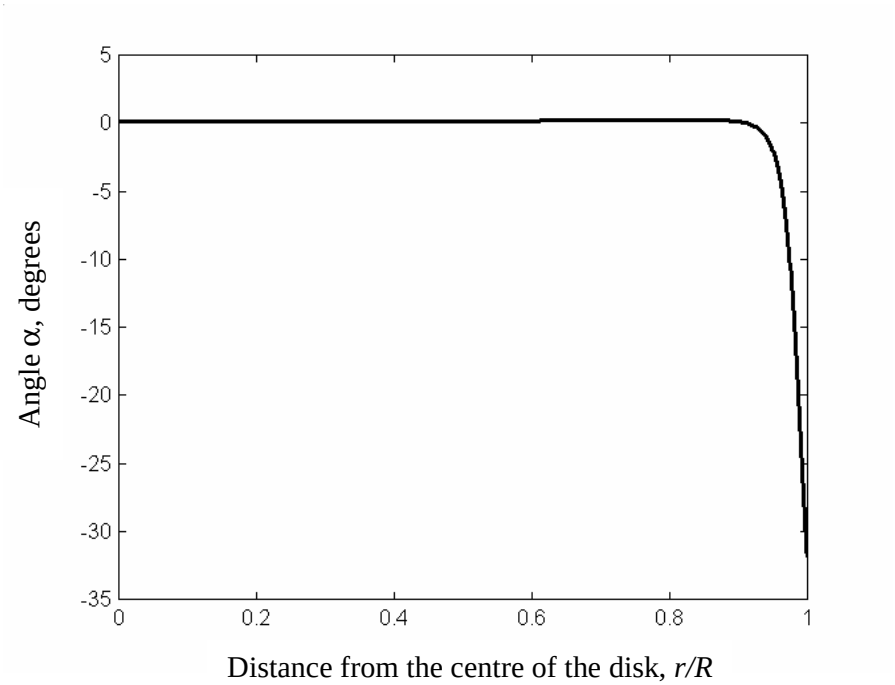

Fig. 7: Angle α between the major principal direction and the *x*-axis vs radius along the main diameter (*P*=-50 MPa; *p*=5MPa; β=11˚; n=4)

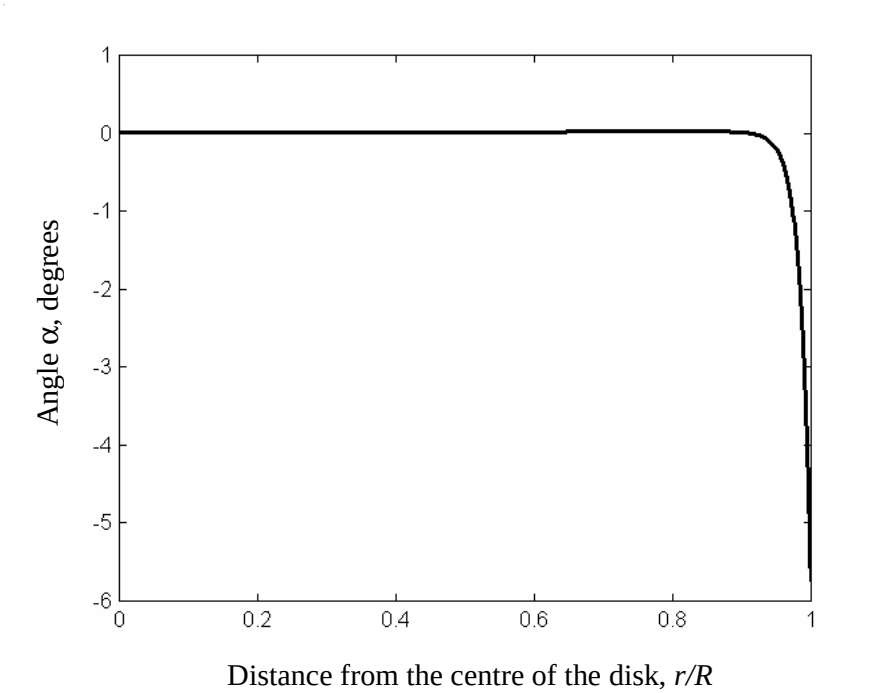

Fig. 8: Angle α between the major principal direction and the *x*-axis vs distance along the main diameter (*P*=-50 MPa; *p*=0.5MPa; β=11˚; n=4)

inside the influence zone in the very vicinity of the loaded arcs remain of the order of p for any value of n. Taking into account the decreasing dimension of the zone, this can produce increasing stress gradients in the vicinity of the loaded arcs. This must contribute to the extensive fracturing usually observed near the loaded parts of the boundary.

5. CONCLUSIONS

A general solution for stress distribution in a disk loaded by radial stresses applied over two opposite arcs of the circular boundary shows that the direction of principal axes in the zones of the main diameter in the vicinity of the loaded arcs can be substantially different from this diameter. For regular oscillations of σ_{rr} given by sine-functions, with increasing frequency of oscillations, the influence zone approaches the loaded arcs, and the maximum deviations from classical solutions in the major part of the disk approach zero. Hence, when calculating stress field in a Brazilian disk, the high-frequency oscillations of the applied radial load can be neglected as it is usually done. Low-frequency oscillations (n of the order of $1 \div 10$ in Eq.(13)) can significantly contribute to the stress distribution and to the orientation of principal axes in the vicinity of the loading platens (Figs. 3 and 7). Their influence on the central part is negligible like the influence of high-frequency oscillations. The results help to explain both relatively consistent fracture mode in Brazilian tests and complicated fracture paths in the contact areas.

Acknowledgements

Thanks are given to Bart Van de Steen for useful discussions. A.Lavrov gratefully acknowledges the support by the Research Council of Katholieke Universiteit Leuven.

References

Bieniawski, Z.T. and Hawkes, I. (1978). Suggested methods for determining tensile strength of rock materials, Int. J. Rock Mech. Min. Sci. and Geomech. Abstr., 15, pp 99-103.

Chen, C.S., Pan, E. and Amadei, B. (1998). Determination of deformability and tensile strength of anisotropic rock using Brazilian tests, Int. J. Rock Mech. Min. Sci. 35, pp 43-61.

Colback, P.S.B. (1966). An analysis of brittle fracture initiation and propagation in the Brazilian test, Proceedings of the First Congress of the International Society of Rock Mechanics, Lisbon, pp 385-391.

Fairhurst, C. (1964). On the validity of the 'Brazilian' test for brittle materials, Int. J. Rock Mech. Min. Sci., 1, pp 535-546.

Jaeger, J.C. and Cook, N.G.W. (1969). Fundamentals of Rock Mechanics, London, Methuen and Co Ltd.

Muskhelishvili, N.I. (1963). Some basic problems of the mathematical theory of elasticity, Groningen, P.Noordhof.

Van de Steen, B. (1999). Boundary element simulations of fracture initiation and propagation in conventional laboratory tests and in diametrically loaded discs containing a stress concentrator, Internal report K.U.Leuven.

Van de Steen, B., Vervoort, A. and Jermei, J. (1998). Crack initiation at a heterogeneity in a rock sample subjected to the Brazilian test, Proc. Intern. Conf. Mechanics of Jointed and Faulted Rock (MJFR-3), Vienna, 4-9 April 1998. Ed.: H.P.Rossmanith. Rotterdam: A.A.Balkema, pp 357-362.

Van de Steen, B. and Wevers, M. (1998). Acoustic emission preceding macro crack formation in samples containing a stress concentrator, Proc. Intern. Conf. Mechanics of Jointed and Faulted Rock (MJFR-3), Vienna, 4-9 April 1998. Ed.: H.P.Rossmanith. Rotterdam: A.A.Balkema, pp 387-392.